J Mater Sci (2011) 46:4034–4045
DOI 10.1007/s10853-011-5332-z

X-ray line broadening and photoelectrochemical studies on CdSe thin films

S. Thanikaikarasan · X. Sahaya Shajan · V. Dhanasekaran · T. Mahalingam

Received: 28 September 2010 / Accepted: 25 January 2011 / Published online: 8 February 2011

Abstract Cadmium Selenide (CdSe) thin films have been prepared on Indium doped tin oxide coated conducting glass (ITO) substrates at various deposition potential and solution pH values using potentiostatic cathodic electrodeposition technique. The deposited films are characterized using X-ray diffraction, scanning electron microscopy, energy dispersive analysis by X-rays, optical absorption, and photoelectrochemical techniques, respectively. X-ray diffraction pattern revealed that the deposited films are found to exhibit hexagonal structure with preferential orientation along (002) plane. X-ray line profile analysis technique by the method of variance has been used to evaluate the microstructural parameters such as crystallite size, rms microstrain, dislocation density, and stacking fault probability. The variation of microstructural parameters with deposition potential, solution pH values, and annealing temperature are studied. Surface morphology and film composition are investigated by scanning electron microscopy and energy dispersive analysis by X-rays, respectively. Optical absorption analysis has been carried out to evaluate the optical parameters such as refractive index, extinction coefficient, real and imaginary dielectric constants, and packing density, respectively. Photoelectrochemical solar cells are constructed using as-deposited and annealed CdSe thin films as photocathode, and their power output characteristics are studied. The experimental observations are discussed in detail.

S. Thanikaikarasan (✉) · X. S. Shajan
School of Basic Engineering and Sciences, PSN College of Engineering and Technology, Tirunelveli 627 152, India
e-mail: S_thanikai@rediffmail.com

V. Dhanasekaran · T. Mahalingam (✉)
Department of Physics, Alagappa University, Karaikudi 630 003, India
e-mail: maha51@rediffmail.com

Introduction

Semiconducting chalcogenides are considered important technological materials due to their wide range of applications in photovoltaic, photodetection, and optoelectronic devices [1–5]. Extensive research has been performed in the last decade to study the preparation and properties of semiconducting chalcogenides. Prospective semiconducting materials for possible photoelectrochemical solar cell fabrication include Cd-chalcogenides which incidentally satisfy most of the requirements for several new electronic and opto-electronic devices such as light emitting diodes, photodiodes, blue green lasers etc. [5, 6]. CdSe is found to be an excellent material with a direct band gap value 1.7 eV which made them interesting for photoelectrochemical solar cells because of its compatibility of band gap with the solar spectrum [7, 8]. Thin films of CdSe are usually crystallized in wurtzite (hexagonal) structure (JCPDS-ICDD, 08-0459) with lattice constants ($a = 4.299$ Å; $c = 7.010$ Å) and in zinc blende (cubic) structure (JCPDS-ICDD, 19-0191) with lattice constant ($a = 6.077$ Å). Perna et al. [3] have prepared CdSe and Zn-doped CdSe (CdSe:Zn) thin films on Silicon (Si) substrates using pulsed laser deposition technique and studied their properties using electrical, structural, optical, photoluminescence, and raman spectroscopic measurement techniques, respectively. Pal et al. [9] have deposited CdSe thin films on glass substrates using vacuum evaporation technique and studied their properties using X-ray line profile analysis, TEM, and TED techniques, respectively. Zhou et al. [10] have prepared CdSe thin films using

chemical deposition technique and studied their structural, morphological, and optical properties. Rouleau and Lowndes [11] have obtained CdSe thin films using sputtering technique and investigated their properties. Preparation of CdSe thin films by hot wall evaporation technique and the variation of microstructural parameters such as crystallite size, strain, dislocation density with respect to film thickness and quartz tube length are investigated by Velumani et al. [12]. Preparation of CdSe thin films using thermal evaporation method and their structural, optical properties have been investigated by Baban and Rusu [13]. When compared to the deposition techniques mentioned above, electrodeposition has emerged as a simple, economical, and viable technique which has been utilized to obtain good quality films for device applications [5, 14]. The attractive features of this method are convenience for producing large area devices, low temperature growth, and the possibility to control the film thickness and morphology by readily adjusting the electrical parameters as well as the composition of the electrolytic solution [5, 14]. Most of the research reports on CdSe thin films have dealt with the qualitative determination of structure type and grain size variation of the deposited films. There are only few reports are available regarding quantitative measurements of microstructural parameters on CdSe thin films. Knowledge about microstructural analysis may provide valuable informations for achieving the optimum growth conditions to obtain good quality films. X-ray line broadening study based on precise measurements upon the position broadening and shape of X-ray profiles on polycrystalline thin films may give valuable informations about the microstructural parameters which determine the microstructural variations in the films. Polycrystalline films with large, strain-free crystallites are obtained for films with sharp line which can be predicted by diffraction theory. In actual experiments, the sharpened lines are not obtained, because the number of physical factors that broaden the pure diffraction line profile. The breadth of the pure profile determines the mean crystallite size, distribution of sizes, and imperfections present in crystal lattice. Hence, an appropriate analysis of line profile should yield information about mean crystallite size, distribution of crystallites, nature, and extent of lattice imperfections. Even though all the above mentioned factors that depend upon line profile. In addition to that, there are some other parameters such as defects (or) dislocations, stacking faults, and strain are also affected by line profile [15]. The microstructural parameters such as crystallite size, rms microstrain, dislocation density, and stacking fault probability are found to influence the physico-chemical properties of deposited films. Moreover, the reduction of stress, dislocation density, and stacking fault probability and increase in value of crystallite size of films may be useful for opto-electronic applications. Pal et al. [9] have investigated the variation of above parameters with respect to film thickness and substrate temperature for vacuum evaporated CdSe thin films. Velumani et al. [12] have reported the variation of above parameters with respect to quartz tube length for hot wall deposited CdSe thin films. However, the variation of above parameters with respect to deposition potential, solution pH, and annealing temperature for electrodeposited CdSe thin films have not been investigated earlier. Hence, we have planned to investigate the variation of above parameters with deposition potential, solution pH, and annealing temperature.

In this study, we have reported our results on the preparation of CdSe thin films on ITO substrates from an aqueous electrolytic bath containing $CdSO_4$ and SeO_2 using potentiostatic cathodic electrodeposition technique. The deposition mechanism has been investigated using cyclic voltammetry. Structural properties of the deposited films are analyzed using X-ray diffraction. X-ray line profile analysis technique by the method of variance has been used to evaluate the microstructural parameters which characterize the microstructural variations in the deposited films. The effect of deposition conditions such as deposition potential, solution pH, and annealing temperature on microstructural parameters are investigated. Also, the morphological, compositional, optical, and photoelectrochemical properties of the films are studied. The experimental observations are discussed in detail.

Experimental details

CdSe thin films were deposited on ITO substrates from an aqueous electrolytic bath containing 0.25 M $CdSO_4$ and 0.0025 M SeO_2. The chemicals used in this study were of Analar Grade reagents. The first working solution of $CdSO_4$ was obtained by dissolving 48.095 g of $CdSO_4$ in 250 cc deionized water. The second working solution of SeO_2 was obtained by dissolving 0.0694 g of SeO_2 in 250 cc deionized water. The solution mixture was formed by mixing 20 cc of the two solutions. This solution mixture was used as an electrolytic bath for all depositions. The pH of the electrolytic bath was maintained in the range between 1.5 and 3.5 by adding an adjustable amount of dilute H_2SO_4 and NaOH. At lower pH values such as below 2.0, adherence of the deposited film to the substrate was very poor. At higher pH values such as above 3.0, precipitation of electrolytic bath occurs which in turn give films with poor crystallinity. Hence, an optimum solution pH value of 2.5 must be fixed to get good quality films with better crystallinity. All the depositions were carried out using a PAR scanning potentiostat/galvanostat unit (EG & G, Model 362, Princeton Applied Research, USA) employing three-electrode

configuration with ITO substrate as working electrode, platinum electrode as counter electrode, and saturated calomel electrode (SCE) as reference electrode, respectively. Before, used for deposition ITO substrates were treated for 15 minutes with ultrasonic waves in a bath of isopropanol and then rinsed with acetone. The SCE was introduced into the solution by luggin capillary arrangement whose tip was placed as close as possible to the working electrode. The deposition potential was fixed in the range between −500 and −900 mV versus SCE using cyclic voltammetry. The films deposited at bath temperature below 50 °C were found to be poorly crystallized, whereas the films deposited at bath temperature above 80 °C, the current densities were found to be higher. These higher current densities suddenly increased the rate of deposition causes peel off of the film from the substrate. Hence, the bath temperature was fixed as 80 °C for all depositions. The solution pH was found to be vary in the range between 1.5 and 3.5. The films deposited at potential, bath temperature, and solution pH values such as −700 mV versus SCE, 80 °C and 2.5 ± 0.1 were annealed in air for 45 minutes at different temperatures in the range between 150 and 450 °C to improve the crystallinity of the deposited films.

Cyclic voltammetric studies were carried out in a standard three-compartment cell using BAS 200A electrochemical analyzer. Thickness of the deposited films was measured using stylus profilometer (Mitutoyo SJ 301, Japan). An X-ray diffractometer (XPERT PRO PANalytical, Netherland) with CuKα radiation ($\lambda = 1.540$ Å) was used to identify the crystalline nature and phases of the deposited films. X-ray line profile analysis technique by the method of variance was used to evaluate the microstructural parameters. Surface morphology and film composition were analyzed using an energy dispersive analysis by X-rays set up attached with scanning electron microscope (JEOL JSM 840). Optical properties of the deposited films were analyzed using an UV-Vis-NIR spectrophotometer (HR-2000, M/S Ocean Optics, USA). Photoeletrochemical measurements were carried out using as-deposited and annealed CdSe thin films as photocathode, platinum electrode as anode, and SCE as reference electrode, and their power output characteristics were investigated.

Results and discussion

Cyclic voltammetric studies

Cyclic voltammetry is a powerful analytical tool for studying the electrochemical reactions in an aqueous electrolytic bath containing $CdSO_4$ and SeO_2. Cyclic voltammetric studies have been carried out in a standard three-compartment cell with ITO substrate as working electrode, platinum electrode as counter electrode, and SCE as reference electrode, respectively. The rate of scanning speed is 50 mV/sec. The voltammetric curves are scanned in the potential region between −1500 and +1500 mV versus SCE. Figure 1 showed the cyclic voltammogram recorded for ITO glass electrode in an aqueous electrolytic bath containing 0.25 M $CdSO_4$ and 0.0025 M SeO_2. It is observed from Fig. 1 that the growth of CdSe starts at a reduction potential −725 mV versus SCE. During cathodic scan, the re-oxidation peak is observed at −450 mV versus SCE which may be due to superimposition of peaks of compound CdSe and element Cd, since this peak is similar to pure solution of $CdSO_4$ and hence no oxidation peak of CdSe is found. A hysteresis is obtained in the potential range between −725 and −695 mV versus SCE indicated that the deposition of CdSe occurred more easily on CdSe surface than those on ITO surface, since the working electrode is actually CdSe instead of ITO [14, 16]. Hence, the deposition of CdSe starts at a more positive potential on the surface of CdSe electrode. The mechanism of formation of CdSe on ITO substrate is described as follows. Since, the reduction of H_2SeO_3 to Se is the rate controlling step in the deposition process; the first process is the reduction of Cd^{2+} to Cd on the surface of the substrate according to Eq. 1 which is followed by electrochemical reduction of $H_2SeO_3^-$ to Se (Eq. 2). Third process is the electrochemical growth of CdSe on ITO substrate Cd according to Eq. 3. Results of cyclic voltammetry showed that the deposition potential in the range between −500 and −900 mV versus SCE is fixed to prepare CdSe thin films.

$$Cd^{2+} + 2e^- \rightarrow Cd \quad (1)$$

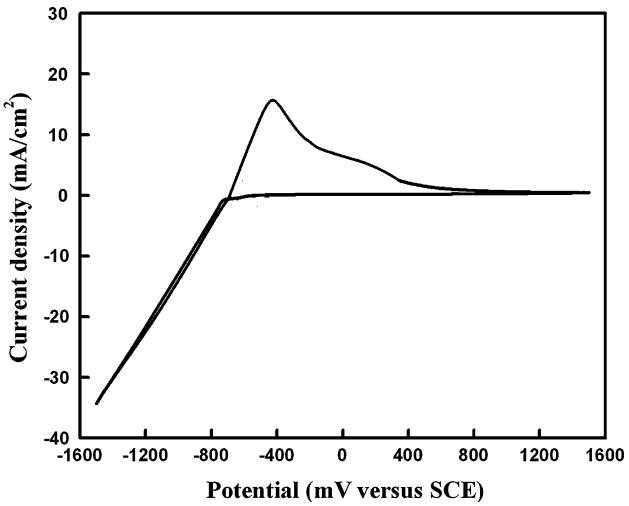

Fig. 1 Cyclic voltammogram of ITO glass electrode in an aqueous solution mixture containing 0.25 M $CdSO_4$ and 0.0025 M SeO_2

$$H_2SeO_3 + 4H^+ + 4e^- \rightarrow Se + 3H_2O \quad (2)$$

$$Cd^{2+} + H_2SeO_3 + 4H^+ + 4e^- \rightarrow CdSe + 3H_2O \quad (3)$$

Film thickness

Thickness of the deposited films is measured using stylus profilometer. The average thickness of the deposited films could be controlled by controlling the plating current and plating time. CdSe thin films deposited on ITO substrates are found to be smooth, uniform, and blackish grey in appearance. The variation of film thickness with deposition time for CdSe thin films prepared at various deposition potentials in the range between −500 and −800 mV versus SCE is shown in Fig. 2. It is observed from Fig. 2a that the film thickness is found to increase linearly with deposition time and tend to attain saturation after 40 minutes of deposition. If the deposition time is increased above 40 min, thickness of the deposited films remains constant up to 60 minutes, thereafter the film thickness is found to decrease slightly not shown in Fig. 2a. Similar trend is observed for films prepared at various deposition potentials. It is also observed that films with lower thickness value are obtained at a deposition potential below −600 mV versus SCE. Films prepared at a potential above −700 mV versus SCE thickness of the deposited films is found to decrease which may be due to the process of hydrogen evolution reaction [14]. Hence, the films prepared in the potential range between −500 and −800 mV versus SCE are found to be uniform, dense, and strongly adhering to the substrates. The maximum value of film thickness is obtained for films prepared at a deposition potential −700 mV versus SCE and at a deposition time of 40 minutes.

Structural studies

X-ray diffraction patterns are recorded for CdSe thin films prepared on ITO substrates at various deposition potentials in the range between −500 and −800 mV versus SCE which is shown in Fig. 3. XRD patterns showed that the deposited films are found to exhibit hexagonal structure with lattice constants ($a = 4.299$ Å; $c = 7.010$ Å). All the identified peaks are from CdSe alloy phase, and hence no peaks corresponding to Cd and Se are present. The different peaks in the diffractogram are indexed, and the corresponding values of interplanar spacing "*d*" are calculated and compared with standard JCPDS-ICDD file for hexagonal CdSe [17]. It is observed from the diffractogram (Fig. 3) that the height of all the peaks are found to increase while increasing the deposition potential from −500 to −700 mV versus SCE, thereafter the height of all the peaks are found to decrease as shown in Fig. 3(d). The height of (002) peak is found to be higher than all other peaks in the diffractogram indicated that the crystallites are preferentially oriented along (002) plane. The presence of sharp and more intense diffraction peaks at a deposition potential −700 mV versus SCE correspond to the formation of polycrystalline morphology of good quality films. The effect of deposition potential on structural properties showed that the deposition potential did not change the structural phase of the deposited films; however, an increase in crystallinity with deposition potential for CdSe thin films are indicated by XRD peaks as shown in Fig. 3. The effect of deposition condition such as deposition potential, solution pH, and annealing temperature on the orientation of polycrystalline thin films are determined by estimating the texture coefficient of the (*hkl*) plane using the following Eq. 4 [18]

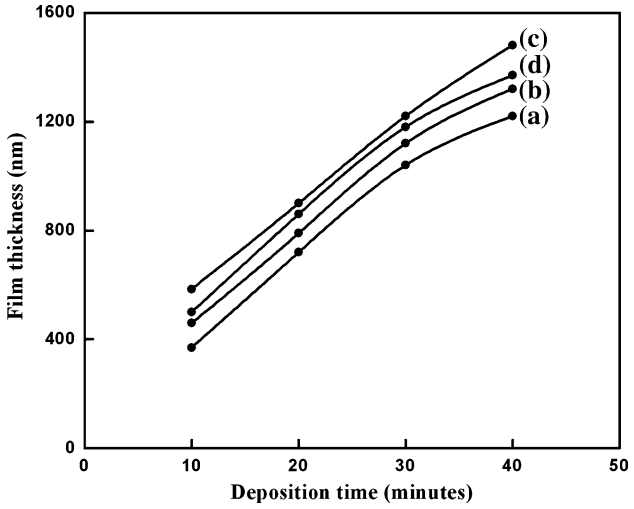

Fig. 2 Variation of film thickness with deposition time for CdSe thin films prepared at various deposition potentials: *a* −500 mV, *b* −600, *c* −700, and *d* −800 mV versus SCE

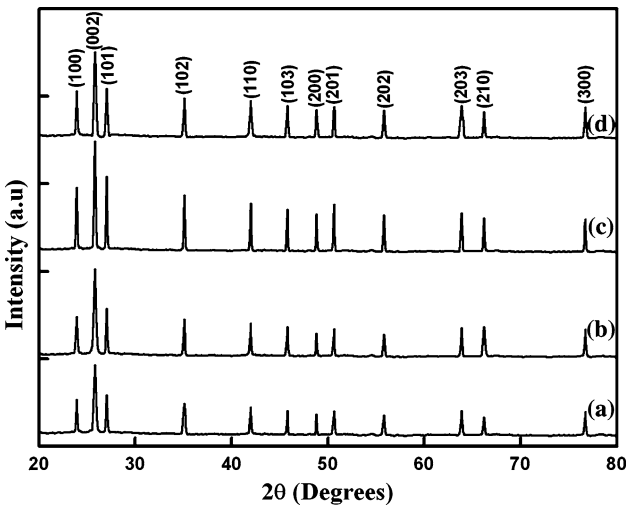

Fig. 3 X-ray diffraction pattern of CdSe thin films prepared at various deposition potentials: *a* −500, *b* −600, *c* −700, and *d* −800 mV versus SCE

$$T_c(hkl) = \frac{I(hkl)/I_0(hkl)}{(1/N)\left[\sum_N I(hkl)/I_0(hkl)\right]} \quad (4)$$

where $T_c(hkl)$ is the texture coefficient of the (hkl) plane, I is the measured intensity, I_0 is the JCPDS-ICDD standard intensity, and N is the number of diffraction peaks. It is observed from Eq. 4 that the value of texture coefficient approaches unity for a randomly distributed powder sample, while $T_c(hkl)$ is greater than unity when the (hkl) plane is preferentially oriented. Figure 4 showed the variation of texture coefficient with (hkl) plane for CdSe thin films prepared at various deposition potentials in the range between −500 and −800 mV versus SCE. It is observed that the texture coefficient is found to increase while increasing the deposition potential from −500 to −700 mV versus SCE, thereafter it is found to decrease slightly as shown in Fig. 4. The films prepared at a deposition potential −700 mV versus SCE have better crystallinity and well adherent to the substrate. The sizes of the crystallites are determined using FWHM data and Debye–Scherrer formula which is given in Eq. 5 [14, 19].

$$P = \frac{0.9\lambda}{\beta \cos\theta_B} \quad (5)$$

For the calculation of crystallite size and rms microstrain the line profiles are subjected to variance analysis method given by Mitra [20]. An aggregate of distorted crystallites as a measure of crystallite size and strain could affect the variation of X-ray diffraction line profiles. Since, the method is sensitive to variation near the tails of the peaks a careful adjustment of the background has been carried out using the method given by Mitra and Misra [21]. For instrumental broadening, the line profiles are corrected by subtracting the variance of the corresponding profile of well-annealed CdSe sample, because of the additive effect of the variance (Fig. 5). Assuming the broadening of the diffracted line is due to crystallite size and strain only, the variance can be written as

$$W_{2\theta} = \left[\frac{\lambda\sigma}{2\pi^2 P \cos\theta}\right] + \left[4\tan^2\theta\langle e^2\rangle\right] \quad (6)$$

where λ is the wavelength of X-rays used, σ the angular range over which the intensity distribution is appreciable, P is the crystallite size, and $\langle e^2\rangle$ is mean square strain. However, the variance is a range sensitive parameter and consequently depends upon the choice of the background level which has a marked influence on the range to be selected for integration. In fact, it is found that the diffraction profiles approach zero, rather asymptotically following an inverse square law according to Eq. 7 (Fig. 6). For such a function varying inversely as the square of the distance from the mean, the variance will be a linear function of the total range σ can be written as

$$W = K\sigma + C \quad (7)$$

Strain is defined as the force which can be act on the surface of the film to restrict the formation of crystallites on the surface of the film. Here, $\langle e^2\rangle^{1/2}$ is the root mean square strain. The rms strain affects the microstructural properties of the deposited films. Dislocation density is defined as the length of dislocation lines per unit volume of the crystal [18, 22, 23]. The dislocation density is calculated using the following Eq. 8

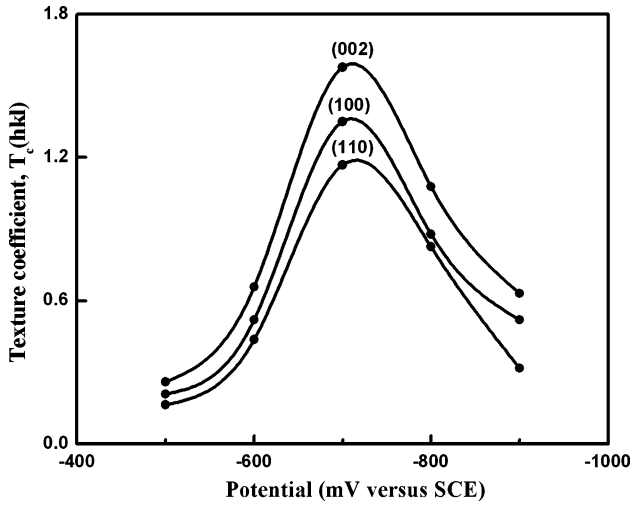

Fig. 4 Variation of texture coefficient along (100), (110), and (002) plane for CdSe thin films obtained at various deposition potentials in the range between −500 and −900 mV versus SCE

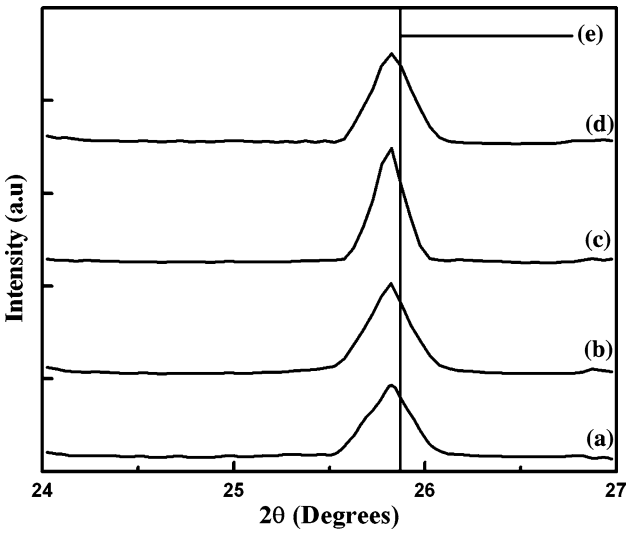

Fig. 5 X-ray diffraction profile showing the peak shift and line broadening: *a* −500, *b* −600, *c* −700, and *d* −800 mV versus SCE. *e Vertical line* indicates the peak position of (002) plane for annealed CdSe thin film

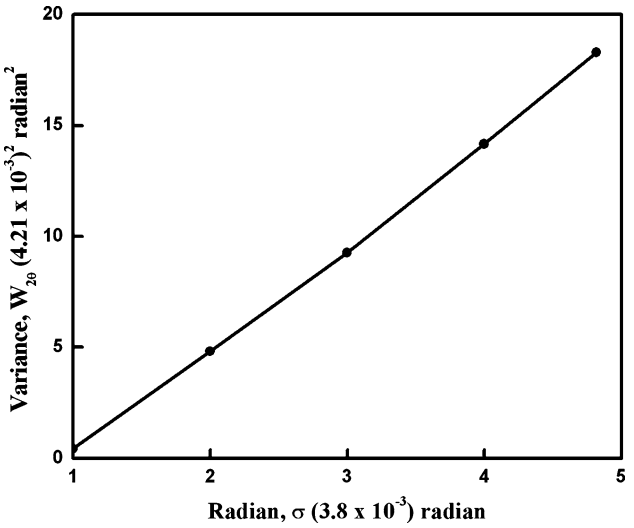

Fig. 6 Plot between range (σ) and variance ($W_{2\theta}$) for CdSe thin films prepared at a deposition potential −700 mV versus SCE

$$\rho = \left[\left(\frac{3nK}{F}\right)^{1/2}\left(\frac{\langle e^2\rangle^{1/2}}{bP}\right)\right] \tag{8}$$

where n be the number of dislocations on each face of the particle, K is constant depending on the strain distribution, F is an interaction parameter, $\langle e^2\rangle^{1/2}$ is the rms strain. For Cauchy strain profile, the value of K is 25, whereas for Gaussian strain profile, the value of K is 4. In the absence of extensive polygonization, dislocation density can be calculated from Eq. 8 by assuming $n = F$, $b = d$, the interplanar spacing and $K = 4$, the above Eq. 8 reduces to Eq. 9

$$\rho = \left[\frac{\sqrt{12}\langle e\rangle^{1/2}}{dP}\right] \tag{9}$$

The stacking fault probability (α) is the fraction of layers undergoing stacking sequence faults in a given crystal, and hence one fault is expected to be found in $1/\alpha$ layers. The presence of stacking faults gives rise to a shift in peak position of different reflections with respect to ideal position of a fault-free well-annealed sample and hence to evaluate the microstructural parameters. Four typical experimental profiles showing the peak shift for hexagonal (002) reflection of CdSe films prepared at different deposition potentials with respect to fault-free well-annealed sample as shown in Fig. 5. A well-annealed powder sample reference is used to compare the shift in peak position of different reflections and hence to evaluate the microstructural parameters. The vertical line in Fig. 5 indicated the peak position of (002) reflection of fault-free well-annealed sample. The relation connecting stacking fault probability (α) with peak shift Δ (2θ) is given by Eq. 10. Using Eq. 10, the stacking fault probability is calculated by measuring the peak shift with the well-annealed sample. A graph is plotted between variance ($W_{2\theta}$) against range (σ) for a typical film of thickness 1480 nm deposited at bath temperature 80 °C is shown in Fig. 6. The emphasis is given here to the points corresponding to the tail because of their great sensitivity towards the variance. The linearity of the graph is confirmed that the background has been adjusted properly, and it also established the correctness of the data.

$$\alpha = \left[\frac{2\pi^2}{45\sqrt{3}}\right]\left[\frac{\Delta(2\theta)}{\tan\theta_{002}}\right] \tag{10}$$

Microstructural analysis

Effect of deposition potential

X-ray diffraction pattern of CdSe thin films prepared at various deposition potentials in the range between −500 and −800 mV versus SCE are recorded. The crystallite size of the deposited films is calculated using FWHM data and Debye–Scherrer formula given in Eq. 5. Using Eq. 6, RMS microstrain is calculated. Dislocation density and stacking fault probability are calculated using Eqs. 9 and 10. Variation of crystallite size and RMS microstrain with deposition potential for CdSe thin films is shown in Fig. 7a. Figure 7b showed the variation of dislocation density and stacking fault probability with deposition potential for CdSe thin films. It is observed that the value of crystallite size is found to increase while increasing the deposition potential up to −700 mV versus SCE, thereafter it is found to decrease slightly as shown in Fig. 7a. The decrease in value of crystallite size above −700 mV versus SCE may be due to the following reason. The deposition potential increases from −500 to −700 mV versus SCE, the strain in the film gets released which in turn increases the crystallite size of the deposited films. If the deposition potential is increased above −700 mV versus SCE, the strain in the film increases slightly which in turn decreases the value of crystallite size as shown in Fig. 7a. Decrease in value of rms microstrain with deposition potential reduced the value of interplanar spacing thus leads to decrease in value of dislocation density and stacking fault probability for films prepared at various deposition potentials (Fig. 7b). The maximum value of crystallite size, minimum value of rms microstrain, dislocation density, and stacking fault probability are noted for films prepared at a deposition potential −700 mV versus SCE. Pal et al. [9] have reported the variation of above microstructural parameters with film thickness and substrate temperature for thermal evaporated

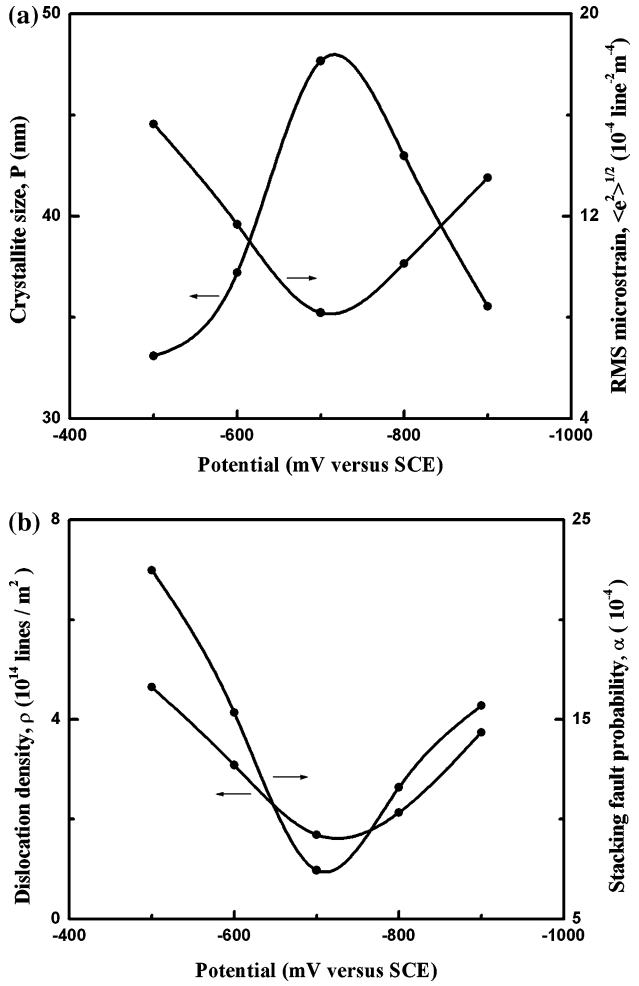

Fig. 7 Variation of **a** crystallite size and rms microstrain **b** dislocation density and stacking fault probability with deposition potential for CdSe thin films

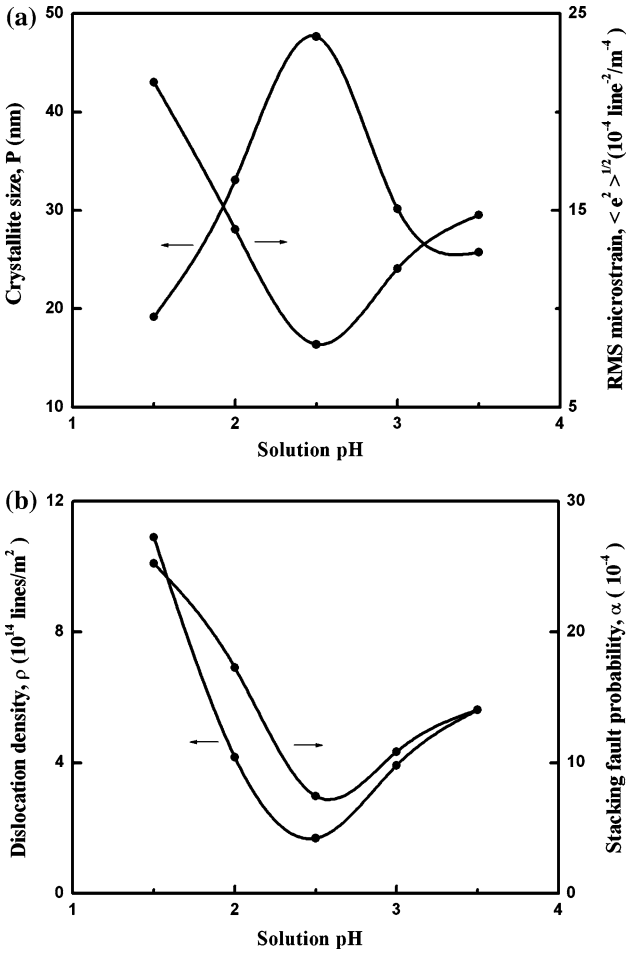

Fig. 8 Variation of **a** crystallite size and rms microstrain **b** dislocation density and stacking fault probability with solution pH value for CdSe thin films

CdSe thin films. The variation of above parameters with respect to film thickness and quartz tube length for hot wall deposited CdSe thin films have been reported by Velumani et al. [12].

Effect of solution pH

X-ray diffraction pattern of CdSe thin films prepared at (deposition potential: −700 mV versus SCE, bath temperature: 80 °C) various solution pH values in the range between 1.5 and 3.5 ± 0.1 are recorded. The crystallite size of the deposited films is calculated using FWHM data and Debye–Scherrer formula. The films deposited at lower pH value such as below 2.0 ± 0.1, adherence of the film to the substrate is very poor. The films prepared at higher pH value such as above 3.0 ± 0.1, precipitation of the electrolytic bath occurred which in turn yield films with poor crystallinity. Figure 8a showed the variation of crystallite size and rms microstrain with solution pH value for CdSe thin films. The variation of dislocation density and stacking fault probability with solution pH value is shown in Fig. 8b. It is observed from Fig. 8a that the crystallite size is found to increase while increasing the solution pH value from 1.5 to 2.5 ± 0.1, thereafter it is found to decrease slightly as shown in Fig. 8a. This may be due to the release of strain in the films which in turn increases the crystallite size of the deposited films. If the solution pH value is increased above 2.5 ± 0.1, precipitation of electrolytic bath occurred which in turn decreases the crystallite size of the deposited films as shown in Fig. 8a. Decrease in value of rms microstrain with solution pH value reduced the value of interplanar spacing thus leads to decrease in value of dislocation density and stacking fault probability for films prepared at various solution pH values (Fig. 8b). The maximum value of crystallite size, minimum value of rms microstrain, dislocation density, and stacking fault probability are obtained for films prepared at a solution pH value 2.5 ± 0.1.

Effect of annealing

CdSe thin films deposited at optimized condition (potential: −700 mV versus SCE, bath temperature: 80 °C, solution pH: 2.5 ± 0.1) are annealed at different temperatures (150–450 °C) in air for 45 minutes, and the effect of annealing on microstructural parameters are analyzed. The process of annealing at higher temperature resulted increase in value of crystallite size of the deposited films. Figure 9a shows the variation of crystallite size and rms microstrain with annealing temperature for CdSe thin films. The variation of dislocation density and stacking fault probability with annealing temperature for CdSe thin films is shown in Fig. 9b. It is observed from Fig. 9a that the value of crystallite size is found to increase while increasing the annealing temperature up to 350 °C, thereafter it is found to decrease slightly as shown in Fig. 9a. If the annealing temperature is increased above 350 °C, there is a marked decrease in the tails of the lines accompanied by a furthermore rapid increase in peak heights. Thus, there is no significant change in lattice parameter during annealing, and small variation in line position must be attributed to experimental errors resulting from removing, annealing, and replacing the same specimen number of times. It is observed from Fig. 9b that both dislocation density and stacking fault probability are found to decrease while increasing the annealing temperature up to 350 °C, thereafter both of them are found to increase slightly. This indicates that an optimum annealing temperature of 350 °C is fixed to obtain CdSe films with suitable microstructural parameters. The process of annealing increases the effective domain size with concomitant decrease in dislocation density of deposited films. The maximum value of crystallite size, minimum value of rms microstrain, dislocation density, and stacking fault probability are noted for films annealed at higher temperature such as 350 °C.

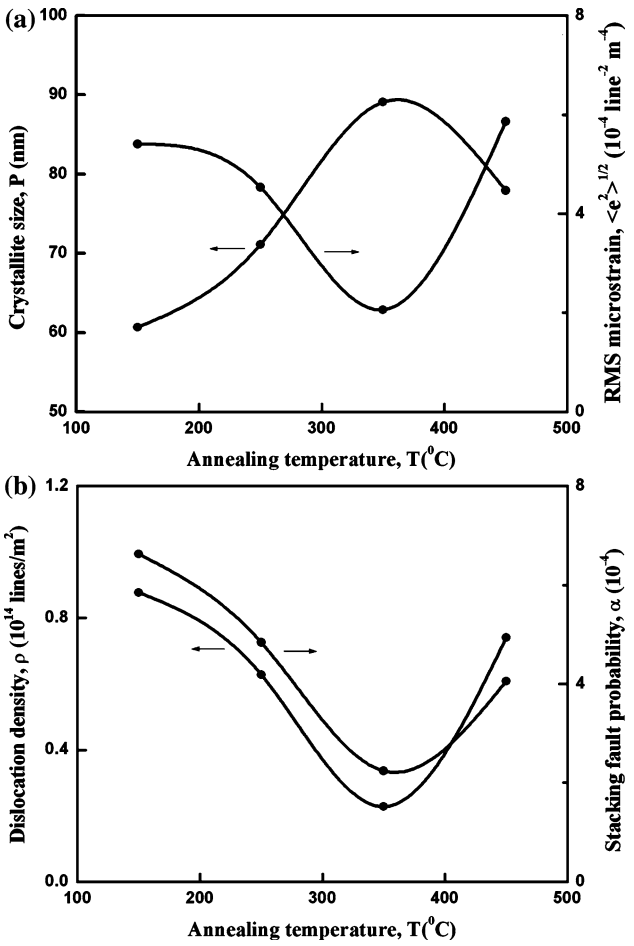

Fig. 9 Variation of **a** crystallite size and rms microstrain **b** dislocation density and stacking fault probability with annealing temperature for CdSe thin films

Morphological and compositional analyses

The surface morphology of CdSe thin films has been analyzed using scanning electron microscope. Figure 10 (a, b) showed the SEM picture of CdSe thin films prepared at two different deposition potentials such as −500 and −700 mV versus SCE. It is observed from Fig. 10(a) that the films prepared at a deposition potential −500 mV versus SCE are found to exhibit island-like structure. There is no definite grain structure that can be easily observed on the surface of the film. The films prepared at a potential −700 mV versus SCE has smooth surface with spherical grains [Fig. 10(b)]. The grains are distributed uniformly over the entire surface of the film. The sizes of the grains are found to be in the range between 0.37 and 0.87 μm. The average size of the grains is found to be 0.69 μm. The film composition has been analyzed using an energy dispersive analysis by X-rays set up attached with scanning electron microscope. Typical EDX spectrum of CdSe thin films prepared at a deposition potential −700 mV versus SCE is shown in Fig. 11. It is observed that the emission lines Cd and Se are present in the investigated energy range represent the formation of CdSe thin films. The variation of Cd and Se content with deposition potential for CdSe thin films prepared at different deposition potentials is shown in Fig. 12. It is observed that the content of Cd decreased and the content of Se increased while increasing the deposition potential from −500 to 900 mV versus SCE. The atomic molar ratio (Cd:Se) for CdSe thin films prepared at a deposition potential is found to be 0.96:1.03 represent the stoichiometric formation of CdSe thin films. This result is consistent with X-ray diffraction analysis of the sample with phase corresponds to CdSe. The EDX value of CdSe thin films obtained at a deposition potential −700 mV is found to be quite closer to the value reported earlier by Datta et al. [24].

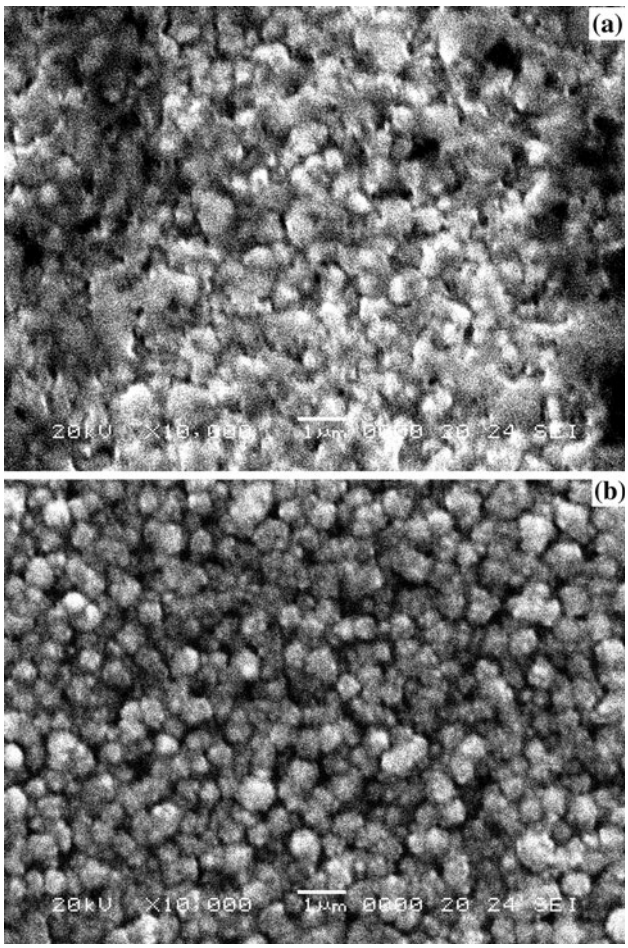

Fig. 10 SEM picture of CdSe thin films prepared at different deposition potentials: **a** −500 and **b** −700 mV versus SCE

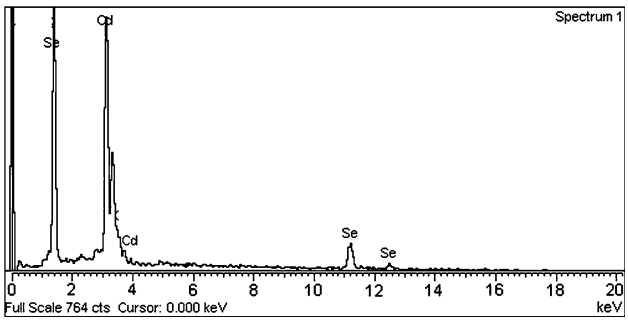

Fig. 11 Typical EDX spectrum of CdSe thin film prepared at a deposition potential −700 mV versus SCE

Optical properties

Optical absorbance and transmittance are recorded for as-deposited and annealed films in the wavelength range between 300 and 1200 nm. The optical band gap is determined from the absorption coefficient value (α) using the following relation [12]

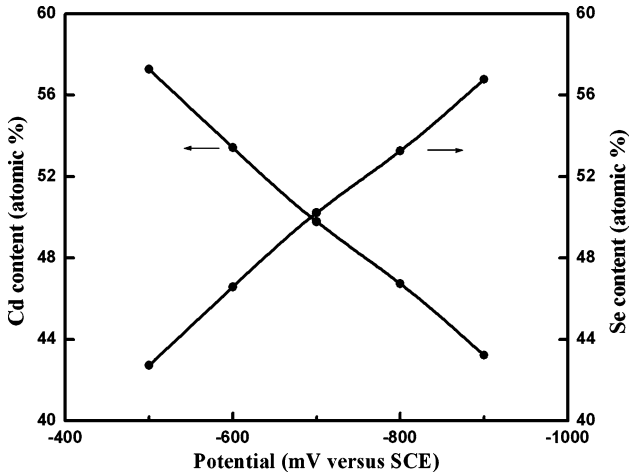

Fig. 12 Variation of Cd and Se content with deposition potential for CdSe thin films prepared at different deposition potentials

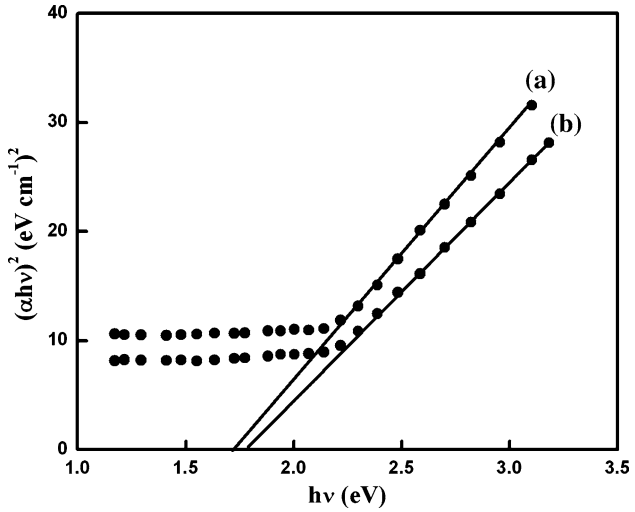

Fig. 13 Plot of ($h\upsilon$) versus $(\alpha h\upsilon)^2$ for CdSe thin films: *a* as-deposited and *b* annealed

$$\alpha h\upsilon = K\left(h\upsilon - E_g\right)^n \tag{11}$$

where α is absorption coefficient, $h\upsilon$ is the photon energy, K is a constant which is related to effective masses associated with the valence and conduction bands, and E_g is the energy gap between the bottom of the conduction band and top of the valence band at the same value of wave vector. The value of n is ½ for allowed direct transition and 2 for allowed indirect transition. An energy gap of 1.73 eV and 1.78 eV is obtained for as-deposited and annealed films by extrapolating the linear portion of the curves to energy ($h\upsilon$) axis as shown in Fig. 13. The deviation in band gap for as-deposited films may due to an excess amount of Se present in the deposited films. The presence of Se introduces a significant fraction of electronic levels in the band gap close to the valence band edge of CdSe, with a

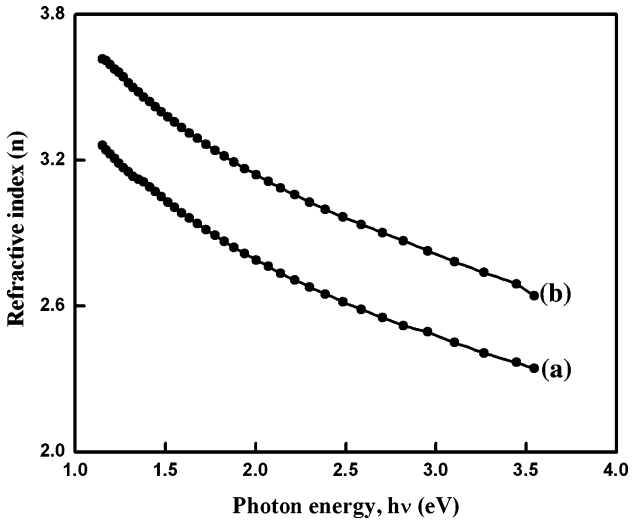

Fig. 14 Variation of refractive index with photon energy for CdSe thin films: *a* as-deposited and *b* annealed

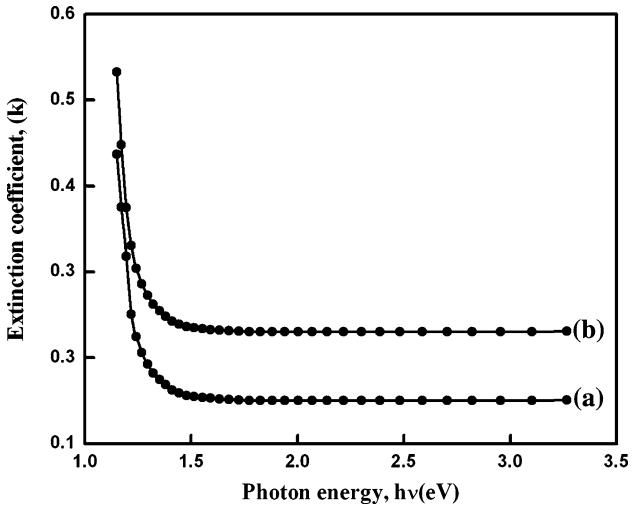

Fig. 15 Variation of extinction coefficient with photon energy for CdSe thin films: *a* as-deposited and *b* annealed

consequent reduction of the energy associated with the direct transition. CdSe films annealed at 350 °C in air for 45 minutes, which remove the excess of unbound Se content in the deposited films. The band gap value obtained in this study is found to be in close agreement with the value reported earlier by Pawar et al. [25]. Figure 14 showed the variation of refractive index (n) with photon energy ($h\upsilon$) for as-deposited and annealed films. Variation of extinction coefficient (k) with photon energy ($h\upsilon$) for as-deposited and annealed films is shown in Fig. 15. It is observed that both refractive index and extinction coefficient are found to decrease with photon energy for as-deposited and annealed films. Variation of real and imaginary (ε_1 and ε_2) dielectric constants with photon energy ($h\upsilon$) for as-deposited and annealed films are shown

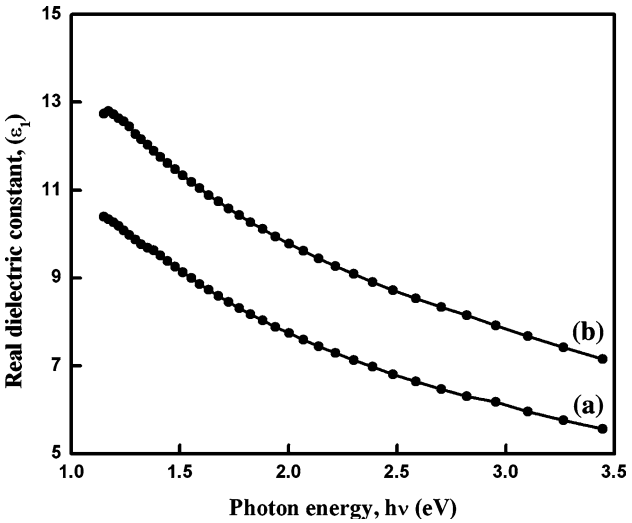

Fig. 16 Variation of real dielectric constant with photon energy for CdSe thin films: *a* as-deposited and *b* annealed

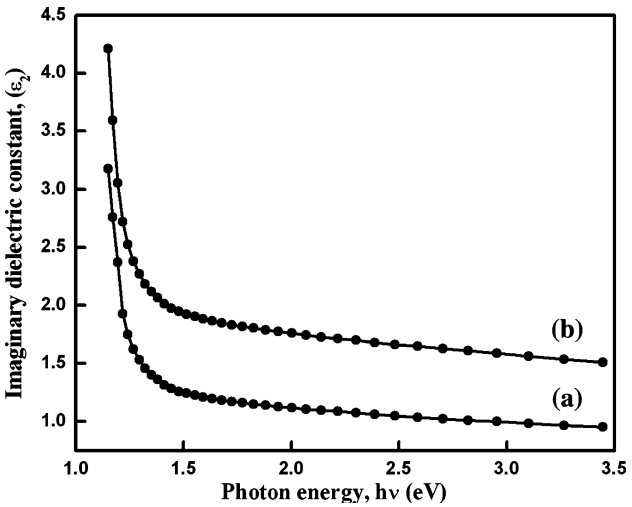

Fig. 17 Variation of imaginary dielectric constant with photon energy for CdSe thin films: *a* as-deposited and *b* annealed

in Figs. 16 and 17. It is observed from Figs. 16 and 17 that both real and imaginary dielectric constants are found to decrease with photon energy for as-deposited and annealed films. Packing density is defined as the ratio of average film density to bulk density. There are various methods are used to relate the refractive index and packing density [26]. The simplest method is linear law of mixing given by Guenther [27]. In this method, the refractive index and packing density are related by the following relation

$$n_f = n_b P + (1 - P) n_v \tag{12}$$

where n_f is the refractive index of the film, n_b is the refractive index of the bulk material, and n_v is the refractive index of voids or pores [28, 29]. In this study, optical

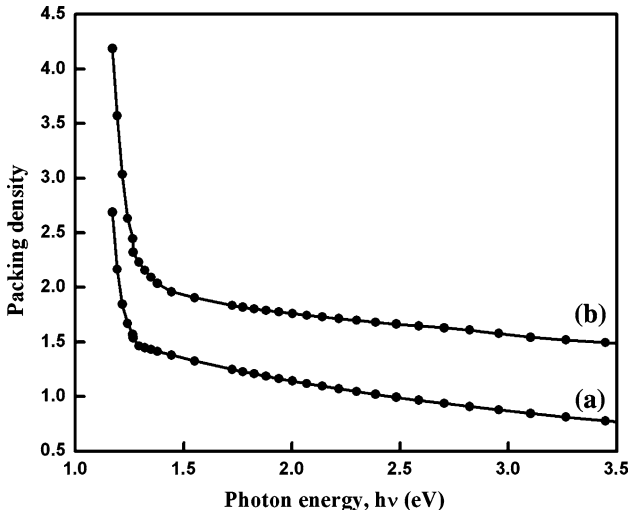

Fig. 18 Variation of packing density with photon energy for CdSe thin films: *a* as-deposited and *b* annealed

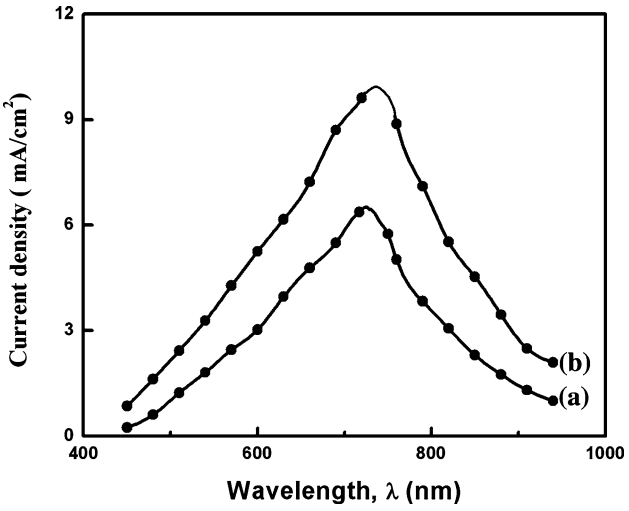

Fig. 19 Variation of photocurrent with wavelength for CdSe thin films: *a* as-deposited and *b* annealed

measurements are carried out in air. It is assumed that the voids in the films are generally filled with moisture. The refractive index of the voids, which may be 1 for empty voids or 1.33 in case of water filled voids [30]. Variation of packing density with photon energy represented that the value of photon energy increases which in turn decreases the packing density as shown in Fig. 18. The value of refractive index, extinction coefficient, real and imaginary dielectric constant, and packing density are found to be higher for annealed films than those for as-deposited films.

Photoelectrochemical properties

Photoelectrochemical solar cells are constructed using as-deposited and annealed film as photocathode, platinum electrode as counter electrode, and SCE as reference electrode, respectively. The solution mixture containing each of 1 M Na_2S, S, and KOH. Figure 19 showed the variation of photocurrent with wavelength for as-deposited and annealed films. Spectral response measurements are carried out in the wavelength range between 300 and 900 nm. It is observed that the photocurrent density is found to increase with wavelength and reaches its maximum value at wavelength 710 and 750 nm for as-deposited and annealed films, respectively. If the wavelength is increased above 710 and 740 nm, the value of photocurrent density is found to decrease as shown in Fig. 19. It is evidenced from Fig. 19 that maximum value of photocurrent density is found to exhibit a peak near the absorption edge of CdSe. Decrease in value of photocurrent density on shorter wavelength region may be due to the recombination of photogenerated carriers caused by surface states [31]. Similarly, decrease in value of photocurrent density on longer wavelength region may be due to transition between

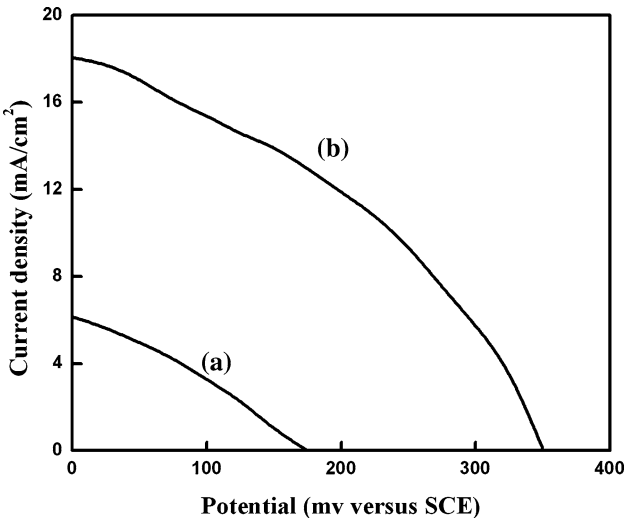

Fig. 20 Power output characteristics of CdSe thin films: *a* as-deposited and *b* annealed

defect levels [32]. Power output characteristics of constructed PEC cells are shown in Fig. 20. The cell parameters such as open circuit voltage, short circuit current density, fill factor, and efficiency are determined from the power output characteristics. The value of efficiency is found to be 0.36 and 2.36 for as-deposited and annealed films. The lower value of efficiency may be due to defect structure of deposited films. The process of annealing at higher temperature such as 350 °C, which remove the defects and the grain size of the fabricated photoelectrodes are found to be high through the fusion of small crystallites. The increase in value of grain size resulted increase in value of diffusion length of charge carriers which enhances the fill factor and efficiency which could be reported by

Moon et al. [33]. Hence, the efficiency of annealed films is found to be higher than those for as-deposited films.

Conclusions

Polycrystalline CdSe thin films have been prepared on ITO substrates using potentiostatic cathodic electrodeposition technique. X-ray diffraction results revealed that the formation of films with hexagonal structure with preferential orientation along (002) plane. Microstructural parameters such as crystallite size, rms microstrain, dislocation density, and stacking fault probability are calculated using line profile analysis, and their dependency with deposition potential, solution pH, and annealing temperature are investigated. Microstructural analysis showed that the microstructural parameters are found to exhibit monotonic variation with deposition potential, solution pH, and annealing temperature. Morphological studies showed that smooth surface with fine grains are obtained for films prepared at a deposition potential −700 mV versus SCE. Stoichiometric films of good quality are obtained at a potential −700 mV versus SCE. Optical properties showed that the parameters such as band gap, refractive index, real and imaginary dielectric constants, and packing density are found to be higher for annealed films than those for as-deposited films due to surface modification of photoelectrode. Photoelectrochemical solar cell studies showed that annealed films have higher efficiency than those for as-deposited films.

Acknowledgement One of the authors (S. Thanikaikarasan) highly thankful to Council of Scientific and Industrial Research (CSIR), New Delhi, India for the award of Senior Research Fellowship(File No. 9/688 (0010) 2008, EMR-I) to carry out this research work. The authors also thanks to DST-FIST for providing X-ray diffraction facilities in Department of Physics, Alagappa University, Karaikudi-630 003, India.

References

1. Hodes G (1995) In: Rubinstein I (ed) Physical electrochemistry: principles, methods and applications. Marcel Dekker Inc., New York
2. Pandey RK, Sahu SN, Chandra Suresh (1996) Handbook of semiconductor electrodeposition. Marcel Dekker Inc., New York
3. Perna G, Capozzi V, Ambrico M, Augelli V, Ligonzo T, Minafra A, Schiavulli L, Pallara M (2004) Appl Surf Sci 233:366
4. Hankare PP, Bhuse VM, Garadkar KM, Delekar SD, Mulla IS (2004) Semicond Sci Technol 19:70
5. Mahalingam T, Thanikaikarasan S, Raja M, Sanjeeviraja C, Lee Soonil, Deak Kim Yong, Sebastian PJ (2007) J New Mater Electrochem Syst 10:33
6. Kirk-Othemer (1982) Encyclopedia of Chemical Technology, vol 20. Wiley, New York
7. Thanikaikarasan S, Sundaram K, Mahalingam T, Velumani S, Rhee Jin-Koo (2010) Mater Sci Eng B 174:242
8. Singh K, Mishra SSD (2002) Sol Energy Mater Sol Cells 71:115
9. Pal U, Samanta D, Ghorai S, Samantaray BK, Chaudhuri AK (1992) J Phys D Appl Phys 25:1455
10. Zhou XW, Lin RF, Xiao XR (1997) Appl Surf Sci 119:203
11. Rouleau CM, Lowndes DH (1998) Appl Surf Sci 127–129:418
12. Velumani S, Narayandass SaK, Mangalaraj D (1998) Semicond Sci Technol 13:1016
13. Baban C, Rusu GI (2003) Appl Surf Sci 211:6
14. Mahalingam T, Thanikaikarasan S, Dhanasekaran V, Mariappan R, Jayamurugan P, Velumani S, Rhee J-K (2010) Mater Sci Eng B 174:249
15. Klug HR, Alexander LE (1974) X-ray diffraction procedures, 2nd edn. Wiley, New York, p 966
16. Shen C, Zhang X, Li H-L (2001) Mater Sci Eng B 84:265
17. Joined Council for Powder Diffracted System-International Centre for Diffraction Data 08-0459, 2003
18. Thanikaikarasan S, Mahalingam T, Raja M, Kim Taekyu, Kim YD (2009) J Mater Sci Mater Electron 20:24
19. Cullity BD (1969) Elements of X-ray diffraction, 2nd edn. Addison-Wesley Publishing Company, Massachusetts
20. Mitra GB (1965) Acta Crystallogr 17:765
21. Mitra GB, Misra NK (1966) Br J Appl Phys 17:1319
22. Williamson GK, Smallman RE (1956) Philos Mag 1:34
23. Hirsch PB (1956) Prog Math Phys 6:236
24. Datta J, Bhattacharya C, Bandyopadhyay S (2006) Appl Surf Sci 253:2289
25. Pawar SM, Moholkar AV, Rajpure KY, Bhosale CH (2006) J Phys Chem Solids 67:2386
26. Harris M, Macleod HA, Ogura S, Pelletier E, Vidal B (1979) Thin Solid Films 57:173
27. Guenther KH (1984) Appl Opt 23:3612
28. Marple DTF (1964) J Appl Phys 35:539
29. Czyzak SJ, Baker WM, Crane RC, Howe JB (1957) J Opt Soc Am 47:240
30. Hale GM, Querry MR (1973) Appl Opt 12:555
31. Frank SN, Bard AJ (1975) J Am Chem Soc 97:472
32. Killedkar VV, Lokhande CD, Bhosale CH (1998) Indian J Pure Appl Phys 36:643
33. Moon H, Kathalingam A, Mahalingam T, Chu JP, Kim YD (2007) J Mater Sci Mater Electron 18:1013